Ceramic Microarrays for Aggressive Environments

Sachin Laddha*, Carl Wu*, Sundar V. Atre*, Shiwoo Lee*, Kevin Simmons**,
Seong-Jin Park and Randall M. German ***

*Oregon Nanoscience and Microtechnologies Institute,
106 Covell Hall, Oregon State University, OR 97330 sundar.atre@oregonstate.edu
**Pacific Northwest National Laboratory, Richland, WA 99354
***Center for Advanced Vehicular Systems,
Mississippi State University, MS 39372, USA

ABSTRACT

Ceramic injection molding (CIM) is a cost-effective technique for producing small, complex, precision parts in high volumes from nanoparticles. To have a good understanding of the CIM process and to provide the necessary data for simulation studies, detailed characterization of the powder-polymer mixture (feedstock) is essential. In this paper, the characterization of feedstocks consisting of alumina nanopowder (average particle size of 400 nm) with ethylene-propylene/wax (Standard Mix) and polyacetal binder systems (Catamold AO-F, BASF) for micro-ceramic injection molding (µCIM) is reported. It was found that the wax-based binder system had lower viscosity and heat capacity as well as greater pseudo-plasticity compared to the polyacetal binder system. However, the results from Moldflow simulations inferred that the Catamold AO-F filled the microcavities (50µm) more efficiently than the Standard Mix.

Keywords: nanoparticles, ceramic microfabrication, powder injection molding, microchannel arrays

1. INTRODUCTION

The role of powder technologies for the net shape production of complex engineering components from metal and ceramic materials continues to grow [1]. One way of net-shaping such components is the use of ceramic injection molding (CIM) which is advantageous as far as shape complexity, materials utilization, energy efficiency, low-cost production, and mass manufacturing are concerned [2].

A major area of application for CIM is in microfluidic systems [3]. Small particles are required for both geometric and performance attributes. Curiously, numerous shape-forming routes for nanoscale powders have been reported which are shown in Figure 1 [3], yet advantages are poorly realized from these powders. In powder systems, the rule of thumb is that the powder size must be smaller than 5% of the feature dimension to reduce wall effects.

Material homogeneity is a critical issue in µCIM because it results in various molding defects in metal or ceramic mircroparts as shown in Figure 2. In this study, an experimental platform and modeling approaches have been used to carry out the research on ceramic microchannel arrays (MCA's) of µCIM.

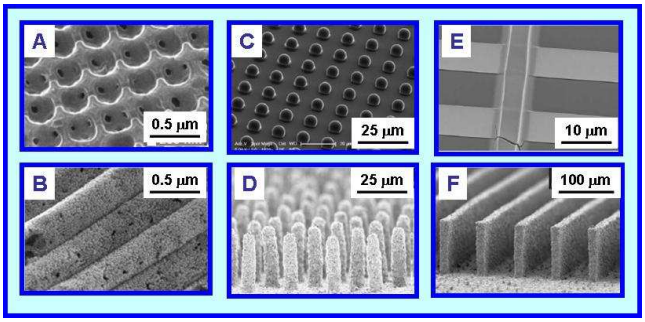

Figure 1: Micromolded nanoparticulate suspensions with 100 nm-20 µm features: (A) SiO_2 photonic bandgap structures, (B) Au nanotube catalysts, (C) SiC tribological microstamps, (D) PZT piezoelectric (E) SnO_2 gas sensors, and (F) Al_2O_3 microfluidic reactor.transducers, (E) SnO_2 gas sensors, and (F) Al_2O_3 microfluidic reactor.

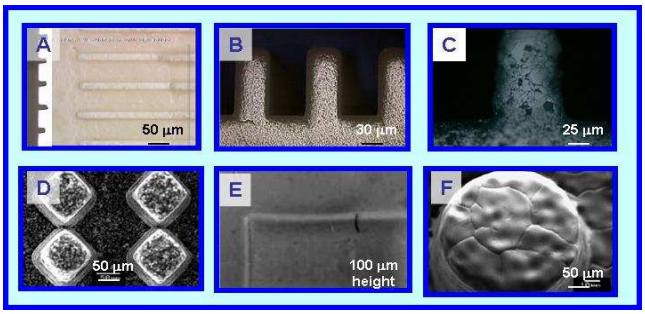

Figure 2: Material inhomogeneity in micromolding nanoparticulate suspensions: [A] incomplete mold fill, [B] ejection crack, [C] porosity distribution, [D] large particle size, [E] bloating during binder removal, and [F] grain growth and cracks during sintering.

The main objective of this research is to investigate the material heterogeneity issue in microcavities through the development of the µCIM process for MCAs. MCAs have been chosen for this study since they have been widely used as the major component and design feature for many microsystems in a large variety of applications, such as microfluidics, micros optics, and micro heat exchangers.

2. EXPERIMENTAL METHODS

2.1 Part Design

Alumina MCA's were designed as the experimental samples for conducting the present study. Figure 3 shows the molded samples of alumina MCA'. The study sample comprised of two structures, the bulk substrate and the microchannel arrays. The bulk size of the small parts with 50μm ribs was 2.5 x 8 x 1.5 mm (width x length x thickness), with an approximate volume of 48 mm^3 and the weight of 0.12g. The small part was also designed with the aspect ratio of 2:1 for the microchannel walls and the large flow path ratio of L/T = 80 (length/thickness).

Figure 3: Alumina MCA's fabricated by μCIM in this study

2.2 Materials

Although there is a relatively wide range of materials available for μCIM, it is necessary to focus on powders of small particle size. The starting powder requirements for μCIM are much more stringent than that used for conventional CIM. For example, the particle size should be at least about one order of magnitude smaller than the minimum internal dimension of the micro part. The feedstocks used in this research are the commercially available alumina-polyacetal feedstock (Catamold AO-F, BASF) and an in-house product, Standard Mix, comprising of alumina-propylene/paraffin wax, both containing about 56 vol.% solids loading. Both these feedstock contain alumina powder A16 SG, supplied by Almatis, with an average diameter of 400 nm.

2.3 Processing

Moldflow software was used to simulate the process. The experiment platform used for micro powder injection molding study consisted of a state-of-the-art PIM machine, ALLROUNDER 270C from Arburg. The machine had a clamping force up to 800 kN. A precision micro mold system was designed with multiple cavities for different MCA with the rib sizes of 50μm. The cavities were designed with gas vents and vacuum paths to improve degassing for fast melt fill, which are critical in the micro injection molding process to reduce voids and micro feature short shot. The cavities were fitted with temperature and pressure sensors to monitor the mold filling

After several trial runs, the basic injection molding process for alumina MCAs was set. Among these process parameters, three of them, volume flow rate, holding pressure and mold temperature were chosen as the DOE control factors to explore the process effects on molded part homogeneity issues.

2.4 Characterization

A few material test methods were explored in this research for studying the green ceramic material homogeneity and mold filling behavior. They include rheological behavior (viscosity), thermal properties (specific heat and thermal conductivity) and pressure-volume-temperature (PVT) behavior.

The rheological characteristics of the feedstock were examined on a Gottfert Rheograph 2003 capillary rheometer at different shear rates and temperatures. The testing was carried out in accordance with ASTM D 3835. The temperatures were between the highest melting temperature and the lowest degradation temperature of the binder system. The barrel of inner diameter of 1 mm and die length as 20 mm was used. The pre-heating time was kept as 6 minutes.

Specific heat measurements were carried out on a Perkin Elmer DSC7 equipment in accordance with ASTM E 1269. The testing was done on 11.85 g of sample with the initial temperature of 190 ^{0}C and final temperature of 20 ^{0}C. The cooling rate was kept constant of 20 ^{0}C/minute.

A K-System II Thermal Conductivity System was used to evaluate the thermal conductivity of the feedstocks. The testing was carried out in accordance with ASTM D 5930. The initial temperature was 190 ^{0}C and final temperature was 30 ^{0}C. The probe voltage was kept as 4 V and acquisition time of 45 s.

A Gnomix PVT apparatus was used to find the PVT relationships of the feedstock materials. The test was carried out in accordance with ASTM D 792. The pellets were dried for 4 hours at 70 ^{0}C under vacuum. The measurement type used was isothermal heating scan with a heating rate of approximately 3 ^{0}C/minute.

3. RESULTS AND DISCUSSION

3.1 Rheological Studies

Figure 4 shows the relation of viscosity versus shear rate at a range of temperatures. The viscosity of both the feedstocks decreases with an increase shear rate and temperature. Further, no dilatant behavior was observed. Normally, feedstocks that exhibit shear-thinning flow behavior during molding ease mold filling and minimize jetting. The rheological data was fitted to a modified Cross-WLF equation and used for further analysis in a Moldflow package.

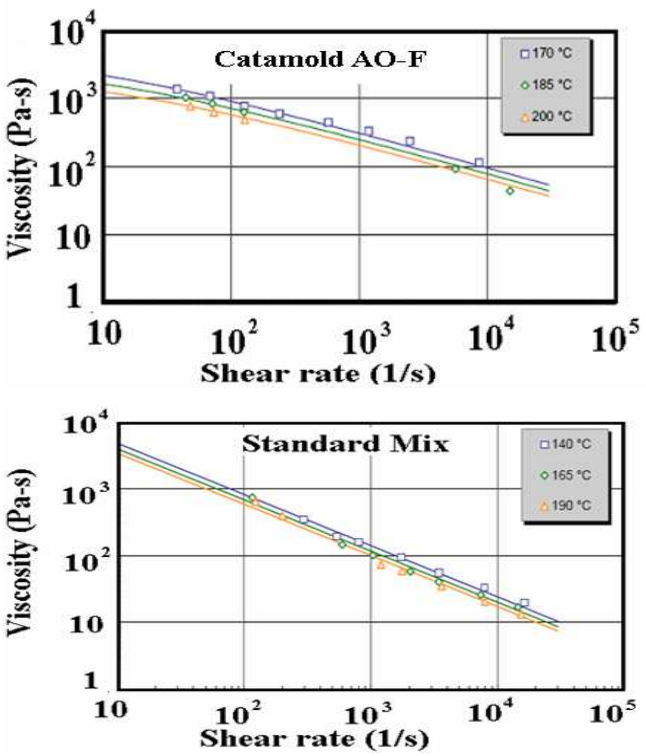

Figure 4: Relationship between viscosity (Pa-s) and shear rate (s^{-1}) for Catamold AO-F and Standard Mix at a melt temperature of 190 ^{0}C.

3.2 Pressure-Volume-Temperature Behavior

The pressure-volume-temperature (PVT) behavior of the Catamold AO- F and Standard Mix (Figure 5), gives the specific volume changes of the melt in cavity as a function of the cavity pressure and temperature. It helps to understand the compression and temperature effects during a typical injection molding cycle. The hold pressure should be chosen after appropriately referring to the PVT-diagram so that the residual cavity pressure is near atmospheric pressure before demolding.

If the hold pressure is too high, the part will still be under pressure when the mold temperature has been reached, which may cause part ejection and relaxation problems. The higher slope in the PVT plot for the Standard Mix (Figure 5) implies a higher tendency for shrinkage in the final part.

3.3 Specific Heat

The Catamold AO-F containing polyacetal has a higher specific heat value compared to the Standard Mix. Figure 6 shows the comparison of the specific heat of the two feedstocks as a function of temperature.

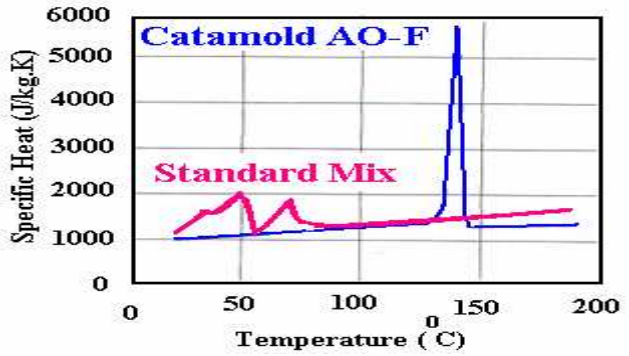

Figure 6: Specific heat (J/kg.K) as a function of temperature for Catamold AO-F and Standard Mix.

3.4 Thermal Conductivity

Figure 7 shows a comparison of the thermal conductivity of the two feedstocks. The Catamold AO-F has a higher thermal conductivity than the Standard Mix. This leads to slower removal of heat from the Catamold AO-F than the Standard Mix during the molding cycle, when the melt and mold temperature are kept constant for both the feedstocks. This can lead to faster and more uniform filling of microchannels for Catamold AO-F compared to the Standard Mix.

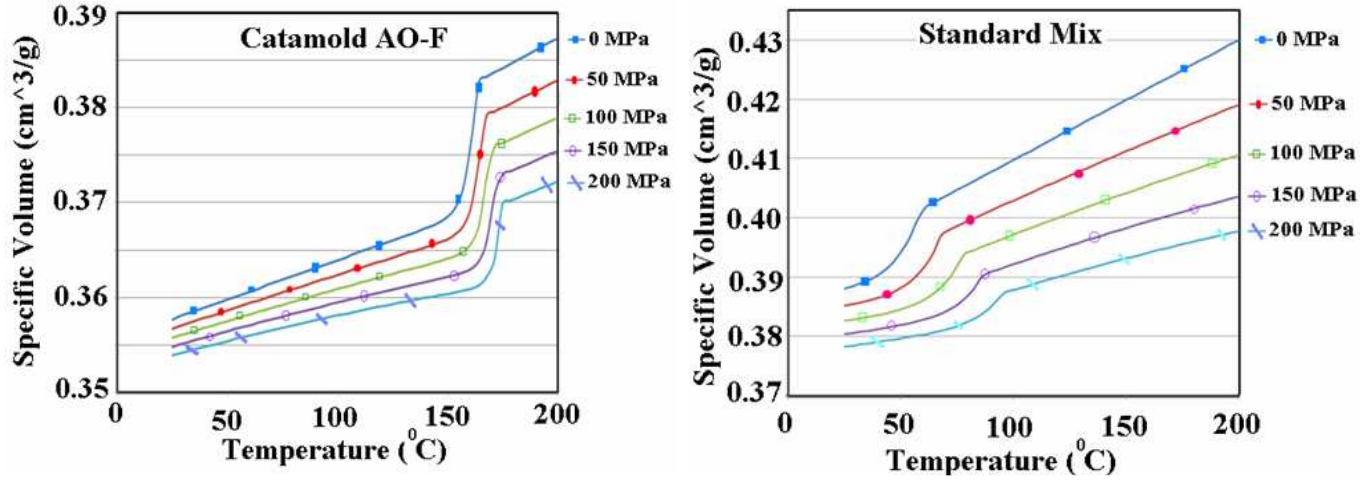

Figure 5: PVT relationships for Catamold AO-F and Standard Mix

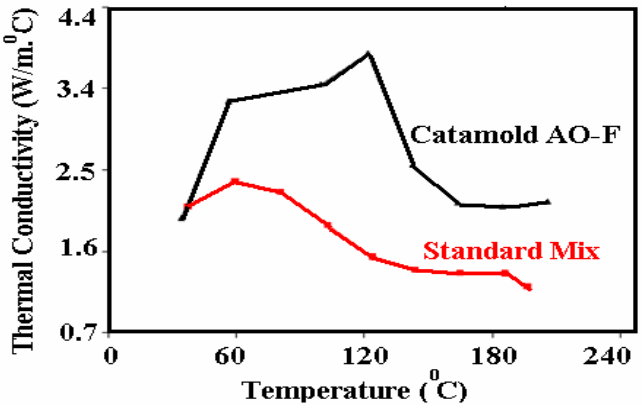

Figure 7: Thermal conductivity of Catamold AO-F and Standard Mix as a function of temperature.

3.5 Progressive filling of microchannels

Figure 8 shows the progressive filling of microchannels using Moldflow simulations for Catamold AO-F at a melt temperature of 190 ^{0}C. Section A in Figure 8 shows that the bulk is filled half way before the microchannels began to fill. Section B and C maintains the same momentum as section A. D shows that all the microchannels are filled at the end of the mold-filling cycle which may cause uneven shrinkage in the part.

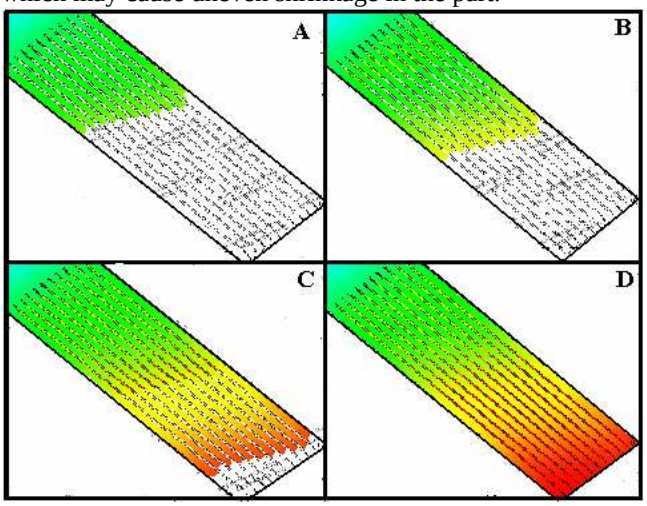

Figure 8: Progressive filling of microchannels using Catamold AO-F at a melt temperature of 190^{0}C from Moldflow simulations.

3.6 Comparison of feedstocks in microchannels

The progressive filling behavior of MCA's discussed in Section 3.5 were quantified and shown in Figure 9. It was found that the amount of feedstock flowing in the microchannels per unit area and per unit time was greater for Catamold AO-F than the Standard Mix. However, the flow in the bulk for both the feedstocks remained nearly the same. This may be due to the difference in thermal and rheological properties of the feedstocks seen in section 3.1 through section 3.4.

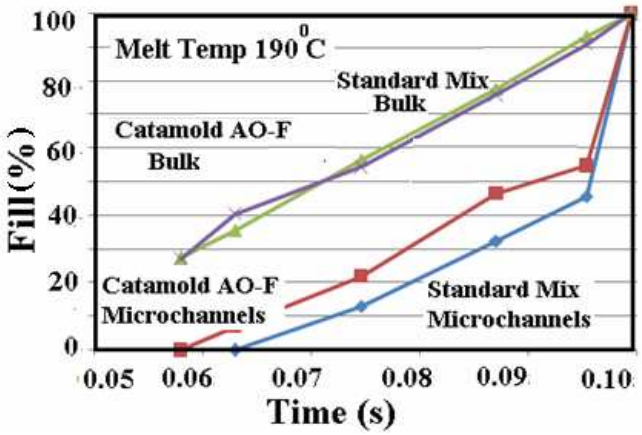

Figure 9: Comparison of Catamold AO-F and Standard Mix in microchannels and bulk at a melt temperature of 190^{0}C

4. CONCLUSIONS

This research emphasizes the effect of polymer on the mold filling behavior of the powder-polymer suspension during the fabrication of MCAs by CIM. It was observed that several material properties determined the mold filling behavior of powder-polymer suspensions. Future work will involve analyzing the influence of mold filling behavior on the occurrence of microscale and macroscale defects.

ACKNOWLEDGEMENT

This material is primarily based on research sponsored by Hewlett-Packard. Additional funding was provided by Air Force Research Laboratory under agreement number FA8650-05-1-5041. The views and conclusions contained herein are those of the authors and should not be interpreted as necessarily representing the official policies or endorsements, either expressed or implied, of Air Force Research Laboratory or the U.S. Government.

REFERENCES

[1] K.F. Ehmann, D. Bourell, M.L. Culpepper, T.J. Hodgson, T.R. Kurfess, M. Madou, K. Rajurkar, and R. E. DeVor "WTEC Panel Report on International Assessment of Research and Development in Micromanufacturing," Based on the findings of a study panel sponsored by NSF, ONR, DOE, and NIST-ATP, October 2005.

[2] R. M. German, *Powder Injection Molding Design & Applications: User's Guide*, IMS Publishers, State College, PA, 2003.

[3] R.A. Saravanan, L. Liew, V.M. Bright, R. Raj, "Integration of Ceramics Research with the Development of a Microsystem," *Journal of the American Ceramic Society*, vol. 86, pp 1217-1219, 2003.